Soft Matter

High-efficient fog harvesting on superhydrophobic microfiber through droplet oscillation and sweeping

Journal:	*Soft Matter*
Manuscript ID	SM-ART-08-2018-001688.R1
Article Type:	Paper
Date Submitted by the Author:	20-Sep-2018
Complete List of Authors:	Zhang, Qiuting; Temple University, Mechanical Engineering Lin, Gaojian; Temple University, Mechanical Engineering Yin, Jie; Temple University, Mechanical Engineering

High-efficient fog harvesting on superhydrophobic microfiber through droplet oscillation and sweeping

Qiuting Zhang, [a] *Gaojian Lin*[a] *and Jie Yin**[a]

[a] Applied Mechanics of Materials Laboratory, Department of Mechanical Engineering, Temple University, 1947 North 12th Street, Philadelphia, PA 19122, USA

*E-mail: jieyin@temple.edu

Keywords: (fog harvesting; superhydrophobic microfiber; water collection; droplet transport; droplet oscillation and sweeping)

Abstract:

Water droplet transport on fibers is of great importance for achieving high water collection efficiency from fog. Here, we exploit a new droplet sliding mechanism to accelerate the droplet coalescence and collection for high-efficient fog harvesting by coating hydrophilic microfibers with superhydrophobic layers of assembled carbon nanoparticles. We find that during the initial water collection, unlike the pinned droplets in axisymmetric barrel shapes wrapping around uncoated microfibers, the hanging droplets on coated microfibers with non-wrapping clamshell shapes are highly mobile due to their lower contact hysteresis adhesion, which are observed to oscillate, coalesce, and sweep the growing droplets along the horizontally placed microfiber. The driving force for droplet transport is mainly attributed to the coalescence energy releasing and fog flow. After introducing a small gravity force by titling coated microfibers with a small angle of 5^o, we find that it can effectively drive the oscillating mobile droplets for directional transport by rapidly sweeping the droplets with a much higher frequency. Finally, the water collection rate from fog on uncoated microfibers over a prolonged duration is found to be improved over 2 times after superhydrophobic coating, and further enhanced to be over 5 times after a small tilting angle of 5^o.

1. Introduction

Harvesting water from fog is often found in nature on fiber-based structures such as slender leaves of trees, spider webs, and cactus spines[1-4]. Inspired by such intriguing phenomena, extensive researches have been conducted to replicating the biomimetic features on fiber structures for fog harvesting[5-7], which has important potential implications in addressing the challenge of water scarcity in arid regions. Based on the wetting of spider web, Jiang's group proposed that artificial bioinspired fibers with spindle knots or humps can be harnessed as good water collectors due to their directional transport of tiny droplets and strong hanging ability[8, 9]. Inspired by the cactus spine, researchers found that conical fibers with curvature gradient and roughness gradient can more efficiently direct the transport of droplets for water harvesting from fog[3, 10]. These studies showed that by tuning the geometry and surface structures of the fibers such as surface roughness variation and curvature gradient, it can induce Laplace pressure difference to overcome the hysteresis adhesion, and drive directional localized transport of tiny droplets to merge into larger ones, which are often pinned to specific sites (e.g. spindle knots or base of conical wire) for water removal under gravity when beyond a critical size[11-13]. Compared with the removal of accumulated pinned droplets by gravity, a dynamic water droplet transporting process without pinning on fibers would potentially dramatically increase the fog harvesting efficiency due to a potential higher water removal efficiency[14, 15], which remains largely unexplored.

Here, we propose harnessing superhydrophobic microfibers with carbon nanoparticle coating for potential high fog harvesting efficiency through dynamic transport of highly mobile droplets. For superhydrophobic curved fiber surface, the motion of droplets is much different from previously reported self-propelled jumping mechanism of droplets on planar superhydrophobic surfaces[16-18]. The effect of surface wetting property of microfibers on the process of water collection is investigated through both experiment and numerical simulation,

including cycles of the static droplet collection and growth, dynamic transport, and successive drop-off of collected droplets. The underlying mechanism governing the droplet configuration formation and dynamic transport of droplets on fibers are qualitatively revealed through both finite element method-based simulation and theoretical analysis. We found that rather than a symmetric barrel shape wrapping around the uncoated hydrophilic microfiber[19-22], the droplets on superhydrophobic coated microfibers exhibit an asymmetric clamshell shape hanging on the bottom surface of fibers with a much lower pinning force, making it more prone to transportation. Different from previously reported self-propelled jumping mechanism of condensed droplets on superhydrophobic flat surfaces or hydrophobic fibers[18, 23-25], we observed an effective dynamic sliding transport mechanism on superhydrophobic coated microfibers through droplets oscillation and coalescence along the microfiber driven by the coalescence energy releasing and environmental perturbation. Finally, the water collection performance over a prolonged duration on both coated and uncoated fibers with different tilting angles are characterized and compared to show the higher efficient water collection through sliding transport mechanism on coated fibers.

2. Experimental Section

Fabrication of superhydrophobic fiber surface*:* The detailed experimental fabrication process of superhydrophobic fiber surface was schematically shown in Supplementary Fig. S1a. A glass slide tilted with 45° was placed in the flame of a paraffin candle. Under it, a silica fiber was held horizontally and rotated continuously 360° to grow assembled carbon nanoparticles-based soots. After growing of 3 minutes, fiber was homogeneously coated with a layer of carbon nanoparticles.

Characterization of fiber morphology*:* A SEM Quanta FEG 450 (FEI Co.) scanning electron microscope was used to characterize the surface morphology of fibers in high vacuum mode

and 10kV acceleration voltage. In Fig S1b, SEM image showed the detailed morphology of coating surface with a high resolution in 500 nm scale bar.

***Characterization of wettability**:* Ramé-hart Model 260 Standard Contact Angle Goniometer was used to measure the contact angle of uncoated and coated glass plates at room temperature of 22°C and relative humidity of 23%. 5 μL deionized water droplets were placed gently onto different sample surfaces. Water contact angles (CAs) were measured by the software. By tilting the sample stage, the contact angle hysteresis was measured at the initial sliding point.

***Water collection performance**:* Fibers were carefully placed horizontally with relative 90% humidity and 18℃ room temperature. The fog flow under the fibers was generated from an ultrasonic humidifier with velocity of 1.5 m/s. The tiny droplets with smaller size (<50 μm) impacted on the fibers. The optical images of water condensation in the initial stage (Figure 2) were taken from Nikon Optiphot-2 Microscope. A high-speed camera with the frame rate of 300 was used to observe the coalescence process within 0.03s in Fig. S2. A Nikon camera was used to record the whole collection process with time.

***Simulation of 3-D shape of a droplet on a fiber**:* The surface energy minimization method implemented in the Surface Evolver (SE) finite element code is used to simulate the 3-D shape of a droplet deposited on a fiber. The total surface free energy (E) associated with the liquid drop with volume V without considering gravity could be expressed as $E = \gamma_{LG}A_{LG} + (\gamma_{SL} - \gamma_{SG})A_{SL} + \iiint(\rho g z)dV$, where g is set to be zero, γ_{LG}, γ_{SL}, and γ_{SG} represent the interfacial tension of liquid-gas, solid-liquid and solid-gas, respectively. The boundary conditions at triple phase contact line includes the constant contact angle and no penetration into rigid cylindrical fiber. At each iteration step, the surface evolver will minimize the total surface free energy E subjected to constraints. The initial shape of simulated condensed water on a fiber is cubic wrapping around fiber. Through continuously minimizing the total surface

energy E, the cubic shape water droplet evolves to a round shape. The iterations stop until a stable total surface free energy is reached. The perturbation is simulated through moving vertices on droplet surface a small distance along the direction perpendicular to fiber. After that, the iteration restart to find the response of droplet shape to the perturbation.

3. Results and discussion

3.1 Wetting on coated and uncoated microfibers

Fig. 1a and 1b show the scanning electron microscope (SEM) images of the surface morphology on smooth silica microfibers (diameter of about 150 μm) with and without coated thin layer of assembled carbon nanoparticles (thickness of about 2 μm). The uniform coating with small roughness (Fig. 1b) was generated through a simple flame synthesis process to render the pristine smooth micro-fibers (Fig. 1a) superhydrophobic, the detailed fabrication process of which is shown in Fig. S1a, where carbon nanoparticles with a typical diameter of 30-40 nm assembled together to form a fractal-like structured surface (Fig. S1b).

To characterize the wettability of fiber surfaces, we quantified the contact angle by measuring the advancing (θ_A) and receding contact angles (θ_R) of the single fiber surface through the Wilhelmy method[26]. It should be noted that it is challenging to measure the contact angle on a fine curling microfiber surface using the sessile drop method. Fig. 1c and 1d showed the side view of apparent contact angle on the coated and uncoated fiber during fog harvesting process. In this process, the fibers are placed in an acrylic chamber with high humidity of 90% at room temperature of 18 ^{o}C. The measurement of contact angles on its counterpart flat coated and uncoated surfaces (Fig. 1e-1f) through sessile drop method are reported as 152° and 35°, respectively, which is consistent with our observation of wetting on microfibers. It indicated that carbon nanoparticle coating could dramatically decrease the wettability of fiber surfaces. Fig. 1g showed that the contact angle hysteresis ($\Delta\theta_{hys}= \theta_A-\theta_R$) decreased from 27^{o} on uncoated fiber to 3^{o} attributed to the carbon-nanoparticle coating layer.

In the following, we would explore harnessing this superhydrophobic fiber coated with carbon nanoparticles for potential high-efficient water collection.

3.2. Wetting effect on fog harvesting on microfibers

We first exploited the initial stage of fog harvesting process on both superhydrophobic (coated) and hydrophilic (uncoated) fiber under high humidity of 90% at room temperature of 18 ^{o}C. Both fibers were placed side by side and horizontally under the microscope for comparison. The fog flow under the fibers was generated from an ultrasonic humidifier with a flow velocity around 1.5 m/s. Fig. 2 showed the time-lapse images of the fog impacting process on both fibers captured under an optical microscope at 10 × magnification during the first 5 second duration. For superhydrophobic coated fiber (on top) under fog flow impact from the bottom, it showed a dropwise fog harvesting mode with numerous tiny micro-droplets (average diameter less than 20 μm) captured on the bottom of the coated fiber during initial water collection. As more water collected, droplets grew larger and coalesced with each other (Fig. 2iv-2vi). Similar to self-removal of microdroplets on superhydrophobic flat surfaces and hydrophobic fibers[18, 27, 28], several droplets were observed jumping away from the superhydrophobic fiber surface due to the surface energy releasing upon droplet coalescence, however, such a phenomenon occurred only in the initial harvesting period under a low super-saturation condition. As collection further proceeded, the initial nonwetting Cassie-Baxter state would transit to the flooded Wenzel state at high super-saturation state with its high contact angle lost. In contrast, for a hydrophilic uncoated fiber (on bottom), it favored a film-wise water collection mode wrapping around the fiber (Fig. 2ii-2iv), which is similar to hydrophilic planar surfaces. Owing to the Rayleigh instability[29], the water film broke up into several individual droplets (Fig. 2v). As droplets further grew larger to a critical value, collected water wrapped around the uncoated fiber (Fig. 2vi). Two typical shapes of a droplet on the fibers were proposed by Carroll and Mchall[20, 22]: asymmetric clamshell shape

and axisymmetric barrel shape. Here, we observed a barrel shape wrapping around the uncoated fiber with a high wettability, while the droplets on the coated fiber were formed in a clamshell shape with a smaller droplet size (Fig. 2vi). During the short duration of fog collection, for both fibers, the effect of gravity on the droplet shape was negligible since the droplet size (diameter less than 200 μm and 520 μm for coated and uncoated fiber) was well below the capillary length of water (2.7 mm)[30].

Next, we investigated the process of accumulation and droplet transport of collected droplets on both coated and uncoated fibers upon prolonged duration of over 120 seconds under high humidity. Fibers with length of 60 mm were fixed horizontally and subjected to a fog flow underneath with a velocity of 1.5 m/s. The prolonged process of fog harvesting and droplet transport on both uncoated and coated fiber surfaces was captured and recorded by a Nikon camera with the representative time-lapse images shown in Fig. 3 and dynamic transport processes shown in the supporting video S1 (uncoated fiber) and S2 (coated fiber). For uncoated fiber (Fig. 3a(i)), we observed a series of uniform barrel-shaped droplets at T = 10 s. As time increases, droplets grew larger in size and broke their symmetric barrel shape to become hung on the bottom side due to the perturbation (Fig. 3a(ii) and (iii)). We also observed that the collected water on the hydrophilic fiber always wrapped around the fiber after growing up to a certain volume (Fig. 3a and Fig. 4a). Further moisture exposure led to the coalesce of neighboring droplets (Fig. 3a(iv)) to form relatively large-sized droplets, which became always pinned on their specific sites (Fig. 3a(iv) – 3a(vi)). Finally, the large-size droplets were removed by gravity overcoming the capillary adhesion (Fig. 3a(vi))[31, 32].

The critical maximum droplet size of stationary droplet to detach can be predicted based on the balance between the gravity and capillary adhesion force given as

$$\rho g V = 4\pi b \gamma \cos(\pi/2 - \beta) \quad (1)$$

where ρ and γ is the water density and surface tension, respectively. b is the fiber radius and β characterizes the asymmetric degree biasing from the center of the fiber. Therefore, the maximum hanging radius on the uncoated fiber can be ideally calculated as 1.1 mm with β approaching to $\pi/2$ and fiber radius of 75 μm, which is slightly larger than the measured value of 0.95 mm at T = 170 s in experiments. A larger fiber radius would increase the hanging drop size (Fig. S2). In contrast, rather than the stationary droplets on hydrophilic uncoated fibers, the superhydrophobic coated fiber favored a dynamic sliding transport of collected droplets along the fiber. Unlike the hanging droplets wrapping around the uncoated fiber, we observed that as fog impacted from the bottom, the collected water droplets on partially wetting coated fiber always hang on the bottom of the fiber without wrapping the fiber on the top even for large volume droplets (Fig. 3b and Fig. 4a). This was evidenced by the fact that a couple of water droplets could still condense on the top of coated fiber with a lower saturation state (Fig. 4a). It would lead to a much lower pinning force due to the relatively smaller contact area when compared to that of hydrophilic fibers. At T = 50 s, droplets with an average radius of 0.6 mm started oscillating randomly and coalescing sequentially (Fig. S3). We believed that the external perturbation such as vibration, air flow, and interaction of water droplets could eventually propel the initial movement of droplets along the fiber. After that, during the process of the horizontal oscillation, the oscillating droplet merged neighboring tiny drops into a larger size and released the coalescence energy to keep transporting the droplets. During this process, coalescence of droplets would efficiently clean up the fiber surface through sweeping. Differing from pinning of droplets on a specific site of uncoated surface, the first detached droplet on the coated fiber was collected at an earlier time of 100 s due to the dynamic oscillation and sliding.

Furthermore, to examine the effect of fog flow rate on the water collection performance on the microfibers, we largely decreased the velocity of the fog flow rate from 1.5m/s to 0.5m/s

in the setup acrylic chamber with 90% humidity. We found that the water collection performance of the coated microfiber is largely decreased due to two major contributing factors. One is the decreasing number of tiny droplets impacted to the fibers per second for potential water collection source; the other is the smaller perturbation force generated from relatively lower air flow rate, which leads to slower oscillations of droplets. Under a slow fog flow rate of 0.5 m/s, for coated fiber (supporting video S3), it shows that the water droplets on coated fibers oscillate in a smaller range and with a lower frequency, resulting a lower efficiency of coalescence of droplets. In addition, the droplets take a much longer time to grow larger in size due to the reduced number of impacted tiny droplets on the microfibers during a slow fog flow. For uncoated microfibers (supporting video S4), since the perturbation of air flow has no effect on the stable pinned droplets, its reduced water collection performance is mainly attributed to the smaller number of impacted droplets on microfibers.

3.3 Theoretical and numerical insights on fog harvesting performance on microfibers

To better understand the underlying mechanism of the droplet sliding on superhydrophobic fiber surface, we qualitatively analyzed the conformation change of hanging droplets under perturbation through finite element simulation at the absence of gravity (see experimental method for more information). Under an idealized condition, the droplet at equilibrium will adopt an axial symmetric barrel shape and its shape is solely determined by the contact angle θ. Here, we chose $\theta = 30^o$ and 90^o to represent the hydrophilic and superhydrophobic wetting state on the fiber, respectively. It should be noted that for an axial-symmetric barrel shaped droplet wrapping around a cylindrical fiber, $\theta = 90^o$ is the maximum contact angle and representing a superhydrophobic state on a fiber. Fig. 4b showed the simulated equilibrium conformations of hanging droplets on a fiber of radius r_f with $\theta = 30^o$ (top) and 90^o (bottom). Both droplets exhibited an axial-symmetric barrel shape, which could be characterized by the

normalized droplet size R_d/r_f and the contact angle θ (top of Fig. 4b). To determine if the equilibrium conformations were stable, we then applied a slight perturbation to the droplet on equilibrium by moving vertices of the droplet surface downward along the direction perpendicular to the fiber with a small distance of 1/10 of the fiber radius to qualitatively simulate the possible perturbation in experiments (Fig. S4). As we can see, such a perturbation broke the axial symmetry of the droplet. For droplets with $\theta = 30^o$, the water droplet still wrapped around the fiber with a relatively larger volume underneath the fiber. In contrast, for droplets with $\theta = 90°$, once the slight perturbation was applied, the whole water droplet tended to move to one side with only a singular point connected to the fiber as shown in the simulation, indicating that the axial symmetric barrel shape on a superhydrophobic fiber was highly unstable. Therefore, in experiments, the external perturbation such as vibration, air flow, and interaction of water droplets could eventually lead to an asymmetrical conformation on superhydrophobic coated fibers. The stability of hanging water droplet in a barrel shape on fibers was theoretically studied by Carrol[19]. He found that for a barrel-shaped water droplet hanging on fiber, it required the normalized radius R_d/r_f to be infinite to ensure a stable barrel shape, which does not exist physically.

The one-side hanging of water droplet could potentially lead to a much higher mobility of water droplet on fiber when compared to the droplets wrapping around the fiber. For the water droplet wrapping around on the uncoated fiber, the two segments of circular triple phase contact line (highlighted with red circles in Fig. 4a) could provide a larger horizontal component of the adhesion force. While for one-side hanging water droplet, the horizontal component of the adhesion force is much smaller compared to that of the droplet wrapping around the fiber since the normal direction of the points on the triple phase contact line is mostly perpendicular to the fiber (bottom of Fig. 4a). Therefore, based on the above analysis,

it explained that it would be much easier for the droplet on superhydrophobic coated fiber to keep sliding with the releasing of coalescence energy.

With the lower contact hysteresis adhesion on superhydrophobic coated fibers, we further explored its potential fog harvesting ability at a small tilting angle of 5^o for gravity driven directional transport and compared with that on uncoated fibers. Fig. 5 showed that similar to the case of horizontal fibers, droplets wrapped around and remained stuck on the tilted uncoated hydrophilic fiber against gravity (supporting video S5). However, by bringing in the gravity force, droplets on the coated fiber could effectively overcome the resistance and slide downward along the fiber with a higher dropping frequency (supporting video S6). In this situation, the critical condition for the drop to slide on the fiber should satisfy the following equation

$$F_r = \rho g V \sin\alpha \quad (2)$$

where F_r represents the force required to move stationary droplet resulting from the surface tension and the contact angle hysteresis, and the right term represents the driving force from the gravity with a tilting angle α. This required moving force has been previously presented by Mead-Hunter et al[33] with

$$F_r = 2\pi r\gamma\left(\int_0^{2\pi} \cos\theta_A \, \underline{\hat{v}} \, d\varphi + \int_0^{2\pi} \cos\theta_R \, \underline{\hat{v}} \, d\varphi\right) \quad (3)$$

where $\underline{\hat{v}}$ is a normalized vector related with droplet shape, r is the radius of contact line, θ_A and θ_R represent the advancing angle and receding angle, respectively[34]. φ is the angular position on the contact line around the fiber. Since the coated fiber surface had a much lower water contact angle hysteresis (the difference between advancing angle and receding angle)[35, 36] compared with that of the hydrophilic surface, a small external force produced by gravity could easily drive the droplets sliding forward by overcoming smaller horizontal component of the contact hysteresis adhesion force, whereas the water droplets remained pinned to the

uncoated fiber despite their large growing size due to the much larger resistance force until their drop-off under gravity when beyond the critical volume in Eq. (1). Therefore, we observed that coated fiber provided a much better performance on the water removal efficiency. At T = 21 s and 31.5 s, the first and second critical drop on the coated fiber swept all the other drops ahead of it in one transport process within a short period of 0.5 s. After that, new tiny droplets collected sequentially and grew on the swept region, which could strongly enhance the water collection efficiency. In contrast, for the uncoated hydrophilic fiber, the detachment of the first drop took a much longer time of 180 s until it grew to the maximum hanging volume. Therefore, the droplet dynamic transport process on the superhydrophobic coated fiber dominated the overall fog harvesting by inducing a higher falling frequency compared with the gravity driven detachment of pinned droplets on specific sites on uncoated fibers.

3.4 Water collection efficiency on microfibers

To quantitatively evaluate the water collection efficiency on fibers, we further investigated the fog harvesting process for a prolonged duration with all conditions unchanged. Fig. 6a shows the comparison of the water collection volume per length between coated and uncoated fibers with and without tilting as a function of collection time over a relatively short period of 5 minutes. It showed that for all the studied fibers, the water collection volume approximately increased linearly with the collection time, the slopes of which were almost the same for both horizontal coated and uncoated fibers, whereas the slope for coated fibers was slightly larger than uncoated ones when tilted. Specifically, for horizontal fibers, the volume of collected water at T = 5min from the coated fiber was over 134 μL, which was twice larger than that collected by the uncoated one. Each dot in the figure represented the collection of one more droplet after detaching from the fibers. Compared to uncoated fibers, the volume of collected water at T = 5min on both coated and uncoated tilted

fibers ($\alpha = 5^o$) became nearly doubled. The reason is that for coated fibers, rather than pinning and drop-off, water droplets would slide directionally along the fiber driven by the combination of coalescence releasing energy and gravitational force. This sliding mechanism led to a much higher falling frequency, as demonstrated by the dense points in the brown dashed line. The water collection volume was dramatically improved by 158% to 320 μL on the coated surface at $T = 5$ min, suggesting an effective way of harnessing nonwetting fiber surface for enhancing the water collection rate due to a higher falling frequency. The water collection performance of fibers with various tilting angles over a much longer duration of up to 5 hours is further compared and the results are summarized in Figure 6b. Inset showed a fiber array with tilting angles changing from 5^o to 30^o. It showed that compared to gradual increasement on uncoated fiber, the water collecting rate on repellent fiber surface was increased dramatically by more than twice at smaller tilting angle (5°) but then flattened out at larger tilting angles. The primary contribution to observed distinction of collecting rate between coated and uncoated fibers was the different contact hysteresis adhesion. For coated fibers, the hysteresis contact angle was measured as 3°, which indicated that small-angle oscillations could lead droplets to immediately sweep through the whole fiber surface, and further increasing tilting angle would have slight effects. In contrast, due to higher hysteresis adhesion (27°) on uncoated fibers, no significant sweeping behavior was observed for uncoated fiber with the highest tilting angle up to 30°. The droplet coalesced with next lower one and stopped at lower point, therefore the collecting rate increased gradually. Generally, the fog harvesting rate was improved by the coating superhydrophobic surface, especially at slightly tilting angle.

4. Conclusion

In conclusion, we demonstrate that by coating hydrophilic microfibers with superhydrophobic layers of assembled carbon nanoparticles, the water harvesting efficiency in

horizontal microfibers from fog can be largely improved over two folds. The introduction of a small tilting angle of 5^o to the coated microfibers can further increase the water collection rate over three folds through directional transport and sweeping along the microfiber. One main contributing factor is that the lower contact hysteresis adhesion on coated microfiber leads to a non-wrapping clamshell shape of droplets, which could result in a sliding mechanism to accelerate the coalescence and sweeping efficiency. Under slight perturbation from environment like air flow and vibration, the faster droplet falling frequency can help dramatically improve the water collection rate. This work provides an important strategy of harnessing superhydrophobic coating on curved fiber surface for potential water harvesting over large areas with a higher collection efficiency.

Conflicts of interest

There are no conflicts of interest to declare.

Acknowledgements

J. Y. acknowledges the funding support from the start-up at Temple University and National Science Foundation (NSF-CMMI-1745921).

References

1. E. B. Limm, K. A. Simonin, A. G. Bothman and T. E. Dawson, *Oecologia*, 2009, **161**, 449-459.
2. Y. Zheng, H. Bai, Z. Huang, X. Tian, F.-Q. Nie, Y. Zhao, J. Zhai and L. Jiang, *Nature*, 2010, **463**, 640.
3. J. Ju, H. Bai, Y. Zheng, T. Zhao, R. Fang and L. Jiang, *Nature Communications*, 2012, **3**, 1247.
4. A. Roth-Nebelsick, M. Ebner, T. Miranda, V. Gottschalk, D. Voigt, S. Gorb, T. Stegmaier, J. Sarsour, M. Linke and W. Konrad, *Journal of the Royal Society Interface*, 2012, **9**, 1965-1974.
5. K.-C. Park, S. S. Chhatre, S. Srinivasan, R. E. Cohen and G. H. McKinley, *Langmuir*, 2013, **29**, 13269-13277.
6. Z. Songnan, H. Jianying, C. Zhong and L. Yuekun, *Small*, 2017, **13**, 1602992.
7. F. T. Malik, R. M. Clement, D. T. Gethin, W. Krawszik and A. R. Parker, *Bioinspiration & Biomimetics*, 2014, **9**, 031002.

8. H. Bai, X. Tian, Y. Zheng, J. Ju, Y. Zhao and L. Jiang, *Advanced Materials*, 2010, **22**, 5521-5525.
9. Y. Hou, Y. Chen, Y. Xue, Y. Zheng and L. Jiang, *Langmuir*, 2012, **28**, 4737-4743.
10. J. Ju, K. Xiao, X. Yao, H. Bai and L. Jiang, *Advanced Materials*, 2013, **25**, 5937-5942.
11. É. Lorenceau and D. Quéré, *Journal of Fluid Mechanics*, 2004, **510**, 29-45.
12. F. Malik, R. Clement, D. Gethin, W. Krawszik and A. Parker, *Bioinspiration & biomimetics*, 2014, **9**, 031002.
13. K.-C. Park, P. Kim, A. Grinthal, N. He, D. Fox, J. C. Weaver and J. Aizenberg, *Nature*, 2016, **531**, 78.
14. D. Seo, J. Lee, C. Lee and Y. Nam, *Scientific Reports*, 2016, **6**, 24276.
15. T. Nørgaard and M. Dacke, *Frontiers in Zoology*, 2010, **7**, 23.
16. K. Zhang, F. Liu, A. J. Williams, X. Qu, J. J. Feng and C.-H. Chen, *Physical review letters*, 2015, **115**, 074502.
17. S. Haefner, O. Bäumchen and K. Jacobs, *Soft matter*, 2015, **11**, 6921-6926.
18. J. B. Boreyko and C.-H. Chen, *Physical Review Letters*, 2009, **103**, 184501.
19. B. Carroll, *Langmuir*, 1986, **2**, 248-250.
20. B. J. Carroll, *Journal of Colloid and Interface Science*, 1984, **97**, 195-200.
21. É. Lorenceau, C. Clanet and D. Quéré, *Journal of Colloid and Interface Science*, 2004, **279**, 192-197.
22. G. McHale, N. A. Käb, M. I. Newton and S. M. Rowan, *Journal of Colloid and Interface Science*, 1997, **186**, 453-461.
23. J. B. Boreyko and C.-H. Chen, *Physics of Fluids*, 2010, **22**, 091110.
24. F. Chu, X. Wu, B. Zhu and X. Zhang, *Applied Physics Letters*, 2016, **108**, 194103.
25. N. Miljkovic, R. Enright, Y. Nam, K. Lopez, N. Dou, J. Sack and E. N. Wang, *Nano Letters*, 2013, **13**, 179-187.
26. B. B. Sauer and T. E. Carney, *Langmuir*, 1990, **6**, 1002-1007.
27. Y. Nam, H. Kim and S. Shin, *Applied Physics Letters*, 2013, **103**, 161601.
28. R. Enright, N. Miljkovic, J. Sprittles, K. Nolan, R. Mitchell and E. N. Wang, *ACS nano*, 2014, **8**, 10352-10362.
29. L. Rayleigh, *Proceedings of the London Mathematical Society*, 1879, **s1-11**, 57-72.
30. P.-G. De Gennes, F. Brochard-Wyart and D. Quéré, in *Capillarity and Wetting Phenomena*, Springer, 2004, pp. 33-67.
31. Z. Huang, Y. Chen, Y. Zheng and L. Jiang, *Soft Matter*, 2011, **7**, 9468-9473.
32. X. Li and Y. Peng, *Applied Physics Letters*, 2006, **89**, 234104.
33. R. Mead-Hunter, B. J. Mullins, T. Becker and R. D. Braddock, *Langmuir*, 2010, **27**, 227-232.
34. D. Quéré, M.-J. Azzopardi and L. Delattre, *Langmuir*, 1998, **14**, 2213-2216.
35. L. Gao and T. J. McCarthy, *Langmuir*, 2006, **22**, 6234-6237.
36. R. E. Johnson Jr and R. H. Dettre, *The journal of physical chemistry*, 1964, **68**, 1744-1750.

Figures and Captions

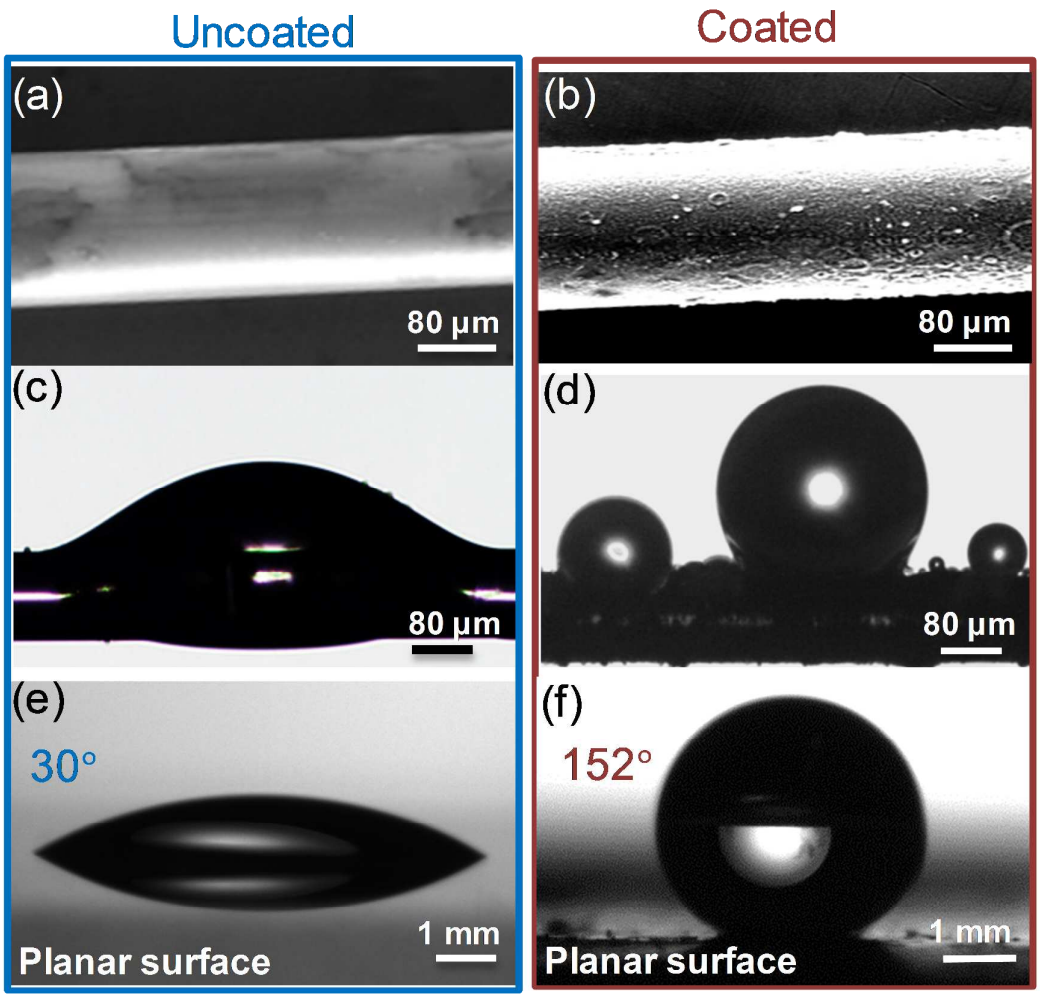

(g)

Surface	$\theta_{adv}(°)$	$\theta_{rec}(°)$	$\Delta\theta_{hys}(°)$
Coated fiber	148	145	3
Uncoated fiber	62	35	27

Figure 1. (a-b) SEM images of surface morphologies on smooth glass microfibers without (a) and with carbon nanoparticles coating (b). (c-d) Apparent contact angle of collected droplets on glass microfibers without (c) and with coated carbon nanoparticles (d). (e-f).Static contact angle of sessile droplets on planar glass surface without (e) and with coated carbon nanoparticles (f).(g) Measured advancing and receding contact angle of coated and uncoated fibers.

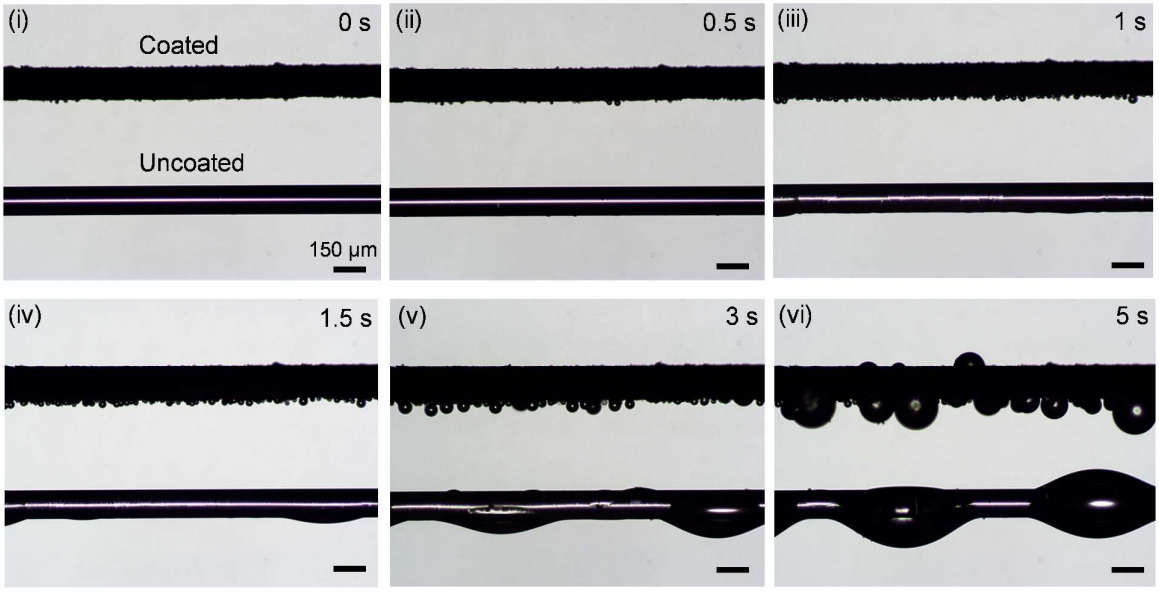

Figure 2. Time-lapse optical images of water condensation process on coated and uncoated microfiber surfaces observed under a microscope during the initial 5 seconds condensation period. On the coated microfiber (top one), numerous tiny droplets nucleated and grew up, while on the uncoated microfiber (bottom one), water film broke into barrel droplets.

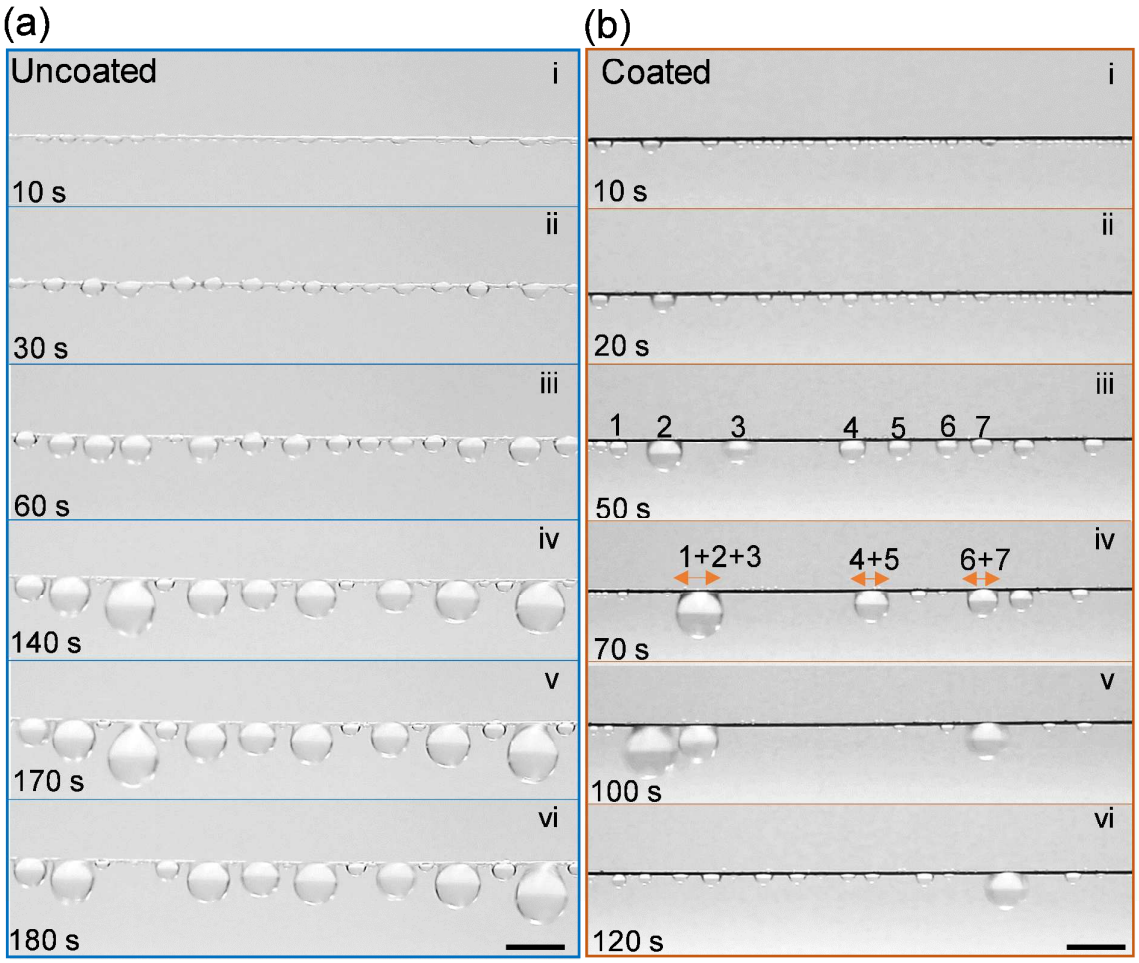

Figure 3. Time-lapse images of a prolonged duration of water coalesce, transport, and falling process on both uncoated (a) and coated microfiber surfaces (b). Condensed water droplets were pinned on specific sites on uncoated microfibers, while oscillating and sliding on coated microfibers.

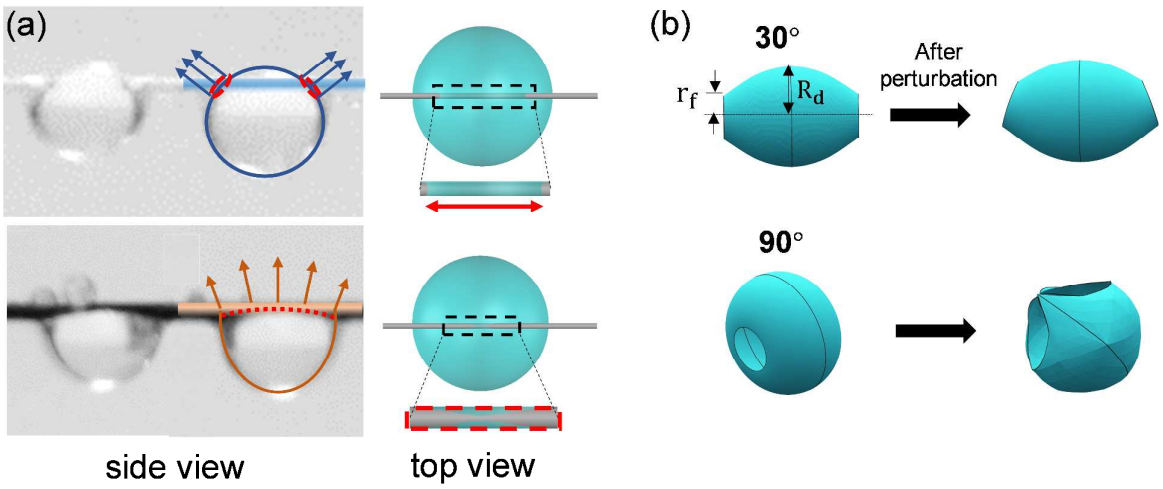

Figure 4. (a) Side and top schematic views of condensed water droplets on uncoated (top) and coated (bottom) microfibers. Red dashed lines represent triple phase contact lines with different directional adhesion force. (b) The simulated equilibrium conformations of axial-symmetric barrel-shaped droplets on fibers with contact angle θ being set to be 30° and 90° (left) to represent a hydrophilic and superhydrophobic wetting state on fiber. After perturbation, the barrel shape becomes asymmetric on hydrophilic fibers whereas it transits to a unstable hanging clamshell shape on superhydrophobic fibers (right).

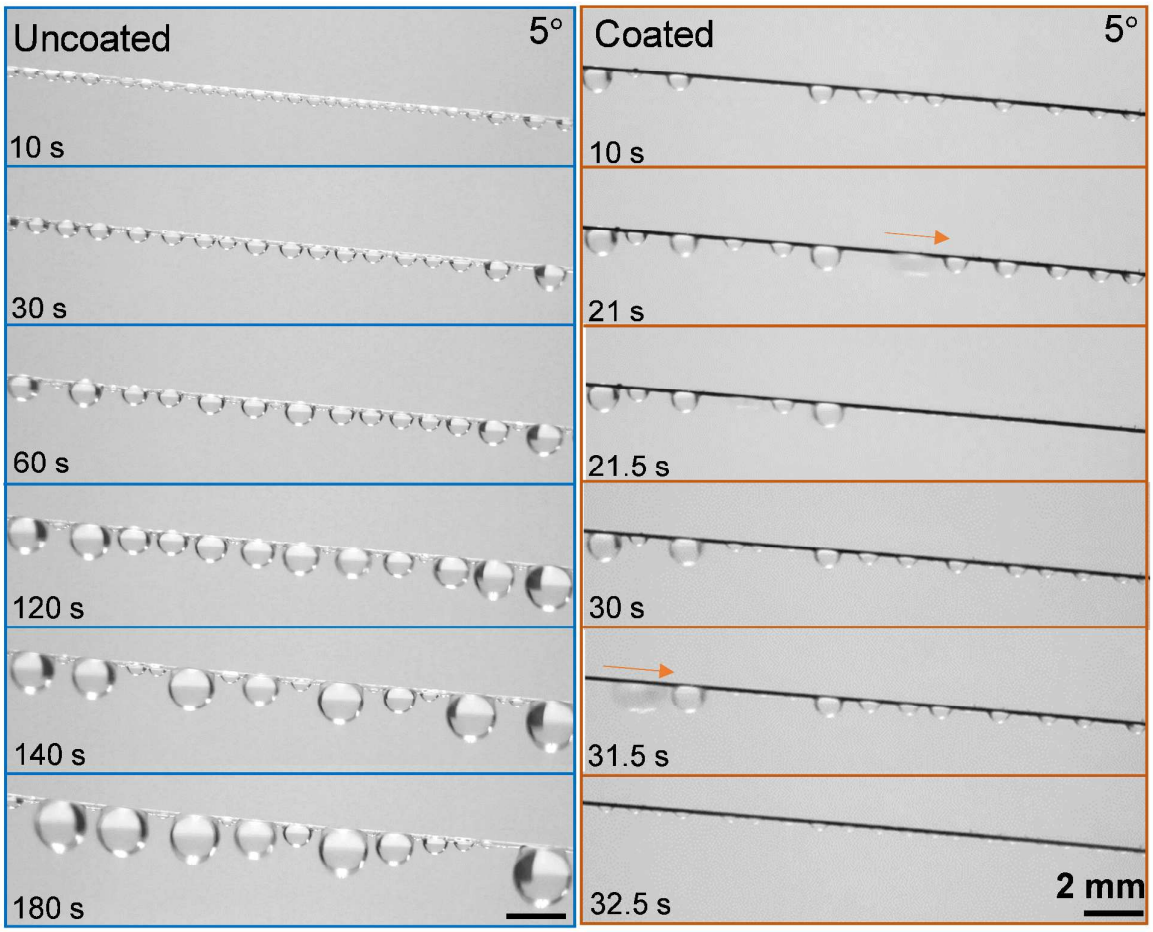

Figure 5. Time-lapse images of water capturing process on both uncoated (a) and coated microfiber surfaces at a small tilting angle of 5° (b). The droplets on uncoated fiber remained pinned on specific sites without sliding. First maximum-sized hanging droplets detached from the microfiber at 180s (a), while a faster collection rate was observed on coated microfibers with droplet sliding and sweeping. (b)

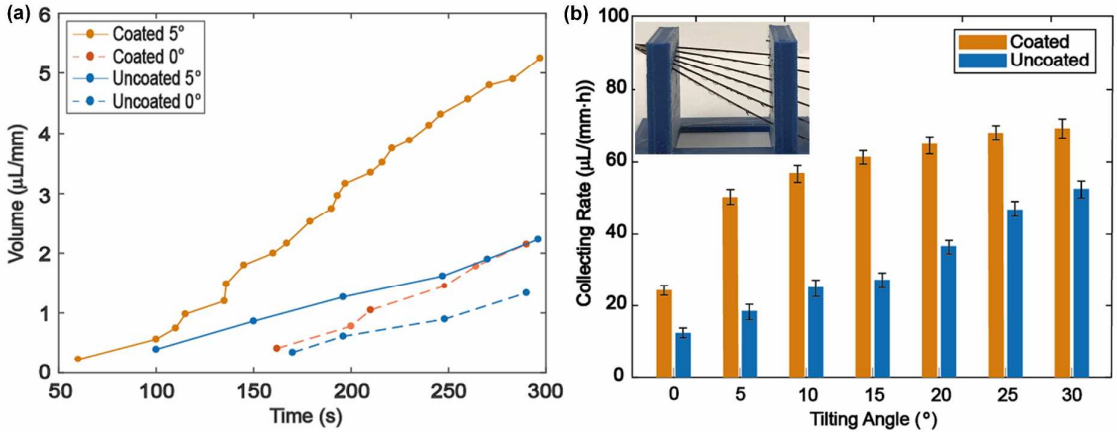

Figure 6. (a) Experimental results of the water collection volume during 5 minutes on coated and uncoated microfibers with and without slight tilting (tilting angel is 5°). (b) Comparison of measured water collection rate over a prolonged duration of 5 hours on coated and uncoated microfibers with various tilting angle.